

Reconfigurable optical channel waveguides in lithium niobate crystals produced by combination of low-dose O^{3+} ion implantation and selective white light illumination

Yang Tan,¹ Feng Chen,^{1,*} Milutin Stepić,² Vladimir Shandarov,³ and Detlef Kip⁴

¹School of Physics, Shandong University, Jinan 250100, China

²Vinča Institute of Nuclear Sciences, P.O. Box 522, Belgrade 11001, Serbia

³Department of Quantum Electronics, State University of Control System and Radioelectronics, Tomsk 634050, Russia

⁴Institute of Physics and Physical Technologies, Clausthal University of Technology, 38678 Clausthal-Zellerfeld, Germany

*Corresponding author: drfchen@sdu.edu.cn

Abstract: We report on a new method to form reconfigurable channel waveguides in lithium niobate crystals, based on a combination of low-dose O^{3+} ion implantation and selective white light illumination. The fabricated structures show low loss as well as rather high resistivity against optical erasure with red or infrared light, while at the same time reconfiguration of the structures remains possible using homogeneous white light illumination. The transmission properties of the channel waveguide modes can be well simulated numerically by the beam propagation method, which allows for the fabrication of tailored optical interconnections.

©2008 Optical Society of America

OCIS codes: (230.7380) Waveguides, channeled; (130.3730) Lithium niobate; (190.5330) Photorefractive optics.

References and links

1. D. Kip, "Photorefractive waveguides in oxide crystals: fabrication, properties, and applications," *Appl. Phys. B* **67**, 131-150 (1998).
2. J.-P. Liu, H.-Y. Lee, H.-F. Yau, Y.-Z. Chen, C.-C. Chang, and C. C. Sun, "One-beam recording in a $LiNbO_3$ crystal," *Opt. Lett.* **30**, 305-307 (2005).
3. Y. Guo, Y. Liao, L. Cao, G. Liu, Q. He, and G. Jin, "Improvement of photorefractive properties and holographic applications of lithium niobate crystal," *Opt. Express* **12**, 5556-5561 (2004).
4. G. Zhang, Y. Tomita, X. Zhang, and J. Xu, "Near-infrared holographic recording with quasi-nonvolatile readout in $LiNbO_3:In,Fe$," *Appl. Phys. Lett.* **81**, 1393-1395 (2002).
5. P. Zhang, D. Yang, J. Zhao, and M. Wang, "Photo-written waveguides in iron-doped lithium niobate crystal employing binary optical masks," *Opt. Eng.* **45**, 074603 (2006).
6. T. Song, S. M. Liu, R. Guo, Z. H. Liu, N. Zhu, and Y. M. Gao, "Observation of composite gap solitons in optically induced nonlinear lattices in $LiNbO_3:Fe$ crystal," *Opt. Express* **14**, 1924-1932 (2006).
7. E. J. Murphy, *Integrated Optical Circuits and Components: Design and applications* (Marcel Dekker, New York, 1999).
8. T. Jansson, "Information capacity of Bragg holograms in planar optics," *J. Opt. Soc. Am.* **71**, 342-347 (1981).
9. D. J. Brady and D. Psaltis, "Holographic interconnections in photorefractive waveguides," *Appl. Opt.* **30**, 2324-2333 (1991).
10. L. B. Aronson and L. Hesselink, "Photorefractive integrated-optical switch arrays in $LiNbO_3$," *Opt. Lett.* **15**, 30-32 (1990).
11. K. Itoh, O. Matoba, and Y. Ichioka, "Fabrication experiment of photorefractive three-dimensional waveguides in lithium niobate," *Opt. Lett.* **19**, 652-654 (1994).
12. P. Zhang, Y. Ma, J. Zhao, D. Yang, and H. Xu, "One-dimensional spatial dark soliton-induced channel waveguides in lithium niobate crystal," *Appl. Opt.* **45**, 2273-2278 (2006).
13. R. Jäger, S.-P. Gorza, C. Cambournac, M. Haelterman, and M. Chauvet, "Sharp waveguide bends induced by spatial solitons," *Appl. Phys. Lett.* **88**, 061117 (2006).
14. E. Fazio, F. Renzi, R. Rinaldi, M. Bertolotti, M. Chauvet, W. Ramadan, A. Petris, and V. I. Vlad, "Screening-photovoltaic bright solitons in lithium niobate and associated single-mode waveguides," *Appl. Phys. Lett.* **85**, 2193-2195 (2004).

15. Herreros and G. Lifante, "LiNbO₃ optical waveguides by Zn diffusion from vapor phase," *Appl. Phys. Lett.* **66**, 1449-1451 (1995).
16. P. D. Townsend, P. J. Chandler, and L. Zhang, *Optical Effects of Ion Implantation* (Cambridge U. Press, Cambridge, 1994).
17. C. Couton, H. Maillotte, R. Giust, and M. Chauvet, "Formation of reconfigurable singlemode channel waveguides in LiNbO₃ using spatial solitons," *Electron. Lett.* **39**, 286-287 (2003).
18. Y. Tan, F. Chen, X. L. Wang, L. Wang, V. Shandarov, and D. Kip, "Formation of reconfigurable optical channel waveguides and beam splitters on top of proton-implanted lithium niobate crystals using spatial dark soliton-like structures," *J. Phys. D* **41**, 102001 (2008).
19. M. Mitchell and M. Segev, "Self-trapping of incoherent white light," *Nature* **387**, 880-883 (1997).
20. Y. Lu, S. Liu, G. Zhang, R. Guo, N. Zhu, and L. Yang, "Waveguides and directional couplers induced by white-light photovoltaic dark spatial solitons," *J. Opt. Soc. Am. B* **21**, 1674-1678 (2004).
21. Y. Gao, S. Liu, R. Guo, X. Zhang, and Y. Lu, "White-light photorefractive phase mask," *Appl. Opt.* **44**, 1533-1537 (2005).
22. F. Chen, X. L. Wang, and K. M. Wang, "Developments of ion implanted optical waveguides in optical materials: A review," *Opt. Mater.* **29**, 1523-1542 (2007).
23. F. Chen, Y. Tan, D. Jaque, L. Wang, X. L. Wang, and K. M. Wang, "Active waveguide in Nd³⁺:MgO:LiNbO₃ crystal produced by low-dose carbon ion implantation," *Appl. Phys. Lett.* **92**, 021110 (2008).
24. G. G. Bentini, M. Bianconi, M. Chiarini, L. Corraja, C. Sada, P. Mazzoldi, N. Argiolas, M. Bazzan, and R. Guzzi, "Effect of low dose high energy O³⁺ implantation on refractive index and linear electro-optic properties in X-cut LiNbO₃: Planar optical waveguide formation and characterization," *J. Appl. Phys.* **92**, 6477-6483 (2002).
25. J. Olivares, G. García, A. García-Navarro, F. Agulló-López, O. Caballero, and A. García-Cabanes, "Generation of high-confinement step-like optical waveguides in LiNbO₃ by swift heavy ion-beam irradiation," *Appl. Phys. Lett.* **86**, 183501 (2005).
26. J. Olivares, A. García-Navarro, G. García, A. Méndez, F. Agulló-López, A. García-Cabanes, M. Carrascosa, and O. Caballero, "Nonlinear optical waveguides generated in lithium niobate by swift-ion irradiation at ultralow fluences," *Opt. Lett.* **32**, 2587-2589 (2007).
27. P. J. Chandler and F. L. Lama, "A new approach to the determination of planar waveguide profiles by means of a non-stationary mode index calculation," *Opt. Acta* **33**, 127-142 (1986).
28. J. E. Goell and R. D. Standly, "Sputtered glass waveguide for integrated optical circuits," *Bell Syst. Technol. J.* **48**, 3445-3448 (1969).
29. J. Shibayama, K. Matsubara, M. Sekiguchi, J. Yamauchi, and H. Nakano, "Efficient nonuniform schemes for paraxial and wide-angle finite-difference beam propagation methods," *J. Lightwave Technol.* **17**, 677-683 (1999).
30. Rsoft Design Group, Computer software *BeamPROP*, <http://www.rsoftdesign.com>.
31. K. Buse, J. Imbrock, E. Krätzig, and K. Peithmann, "Photorefractive effects in LiNbO₃ and LiTaO₃," in *Photorefractive Materials and Their Applications 2: Materials*, P. Günter and J.-P. Huignard, eds. (Springer, New York, 2007).

1. Introduction

Light-induced refractive index changes in photorefractive lithium niobate (LiNbO₃) crystals, which are known as self-defocusing media, can be realized at power levels of milliwatts or even lower, which makes this material favorable for many photonic applications, including data storage, optical signal amplification, etc. [1-4]. Recent research reveals that such photo-induced index modifications could be utilized for the fabrication of reconfigurable optical waveguides (in both planar and channel configuration), or for the design of compact integrated photonic devices, e.g. Y-branches, by applying coherent laser beam writing (for example, by using either lithographic masks [5] or multi-beam interference patterns [6]). Compared with planar waveguides, channel waveguides are favorable because these two dimensional (2D) compact structures can carry higher optical intensities, and, in most cases, can be much easier connected with other optical components in modern optical systems based on fiber technology [7].

Reconfigurable optical interconnections in photorefractive LiNbO₃ waveguides have been proposed using thick holograms written by external light beams [8,9]. Dynamic interconnections have been also demonstrated by Hesselink's group, who used two sets of channel waveguides crossing at 90° angles inside an Fe:LiNbO₃ sample [10]. Alternatively, optical connections can be fabricated by scanning an external focused light beam to record channel waveguides inside a bulk LiNbO₃ sample [11]. By using spatial solitons (via

photovoltaic or screening mechanisms), 2D optically induced channel waveguides have been reported in LiNbO₃ [6, 12-14]. Another solution of forming 2D waveguides in this crystal is using selective light illumination on top of a planar waveguide substrate (produced by other techniques, e.g., metal ion in-diffusion [15], or ion implantation [16]). In this way, light will be confined in two dimensions: vertically by the original planar waveguide, and laterally by the light-induced refractive index changes. For example, Couton *et al.* reported single-mode channel waveguide formation in Fe:LiNbO₃ on top of a titanium-diffused slab waveguide using photovoltaic dark solitons formed with coherent green light [17]. Recently, we reported on reconfigurable channel waveguides and Y-branch beam splitters by using dark-soliton like structures superimposed on a proton implanted planar waveguide in Fe:LiNbO₃, in which a green laser at wavelength 532 nm was also employed to selectively illuminate the sample surface through a specially designed photo mask [18]. Although the coherent light from lasers is usually used for the fabrication of such channel waveguides, incoherent broad light sources (e.g., incandescent light bulbs) are more attractive because of the much lower costs [19]. Particularly, it has been shown that incoherent white light can induce refractive index changes in LiNbO₃ [20,21], which implies much easier solutions to form photo-induced waveguide structures in this crystal by utilizing various white light sources instead of coherent lasers.

As one of the most efficient techniques for material modification, ion implantation has been used to successfully produce optical waveguides in a large number of substrates [22]. Recent research has shown that, compared with light-ion (e.g., H or He) implanted LiNbO₃ waveguides, the heavy-ion (e.g., C, O, F or Cl) implanted structures show superior transmission quality and low losses [23-26], mainly related to the used doses for heavy ions which are 1-3 orders lower than those for light ions. In this work, we report, for the first time to our knowledge, on the fabrication of reconfigurable channel waveguides in Fe:LiNbO₃ crystals produced by combination of low dose O³⁺ ion implantation (for light confinement within a planar layer) and selective white light illumination (for lateral confinement). One advantage of this method is that, due to the small thickness of the ion-implanted planar waveguide (less than 5 μm), white light induced structures only need to maintain their spatial shapes within several microns without broadening laterally, which does not require a thoroughly non-diffractive structure formation throughout the crystal, i.e., when forming a spatial soliton.

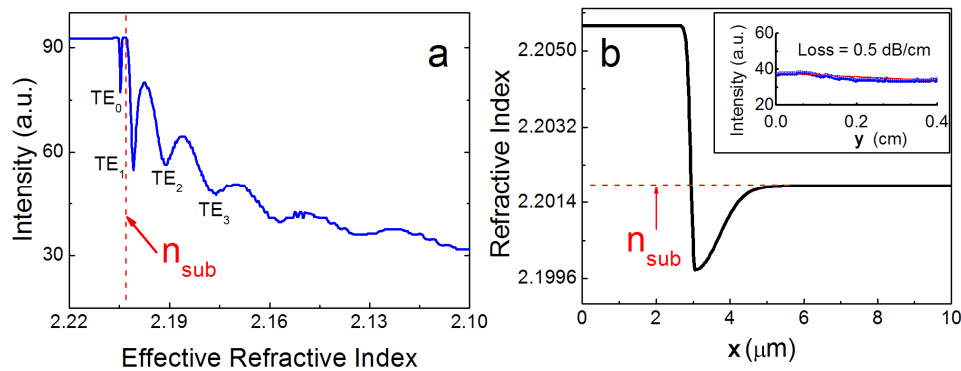


Fig. 1. (a) Dark mode spectrum and (b) reconstructed n_e profile of the O³⁺ implanted planar waveguide in Fe:LiNbO₃. The substrate index n_{sub} is marked for comparison. The inset in (b) shows the scattered light intensity spectrum extracted from the sample surface versus the propagation length in y -direction of the sample.

2. Results and discussion

The x -cut Fe:LiNbO₃ (doped with 0.1 mol% Fe) wafer has dimensions of $2(x) \times 10(y) \times 7(z)$ mm³. As a first step, one optically polished face (with dimensions of 10×7 mm², where the ferroelectric c -axis points along the 7 mm side) is implanted by 6 MeV O³⁺ ions at a dose of 2×10^{14} cm⁻² using the 2×1.7 MV tandem accelerator at Peking University. After annealing at

260°C for 30 min in air to reduce the influence of generated electronic defects in the implanted layer, a planar waveguide layer is formed on top of the sample surface. Figure 1(a) shows the dark mode (or m-line) spectrum for TE modes of the waveguide at 632.8 nm through a prism coupler (Model 2010, Metricon, USA). As one can see, the first mode TE₀ has a larger effective refractive index (n_{eff}) than that of the substrate (n_{sub}), whilst the n_{eff} of three additional modes are lower than n_{sub} . We reconstructed the extraordinary refractive index (n_e) profile by reflectivity calculation method (RCM) [27] according to the dark mode spectrum [Fig. 1(b)]. The measured thickness of the waveguide ($x \approx 3\mu\text{m}$) is in good agreement with the mean projected range of the incident O³⁺ ions. As one can see, this waveguide is confined by a positive index well (with index change $\Delta n_e \approx +0.0038$) and a negative optical barrier with index change of $\Delta n_e \approx -0.002$ at a depth of $x \approx 3.1\mu\text{m}$. The propagation loss of the TE₀ mode of the planar waveguide is determined to be $\sim 0.5\text{ dB/cm}$ at 632.8 nm, which is measured by the scattering detection technique [see inset of Fig. 1(b)] [28].

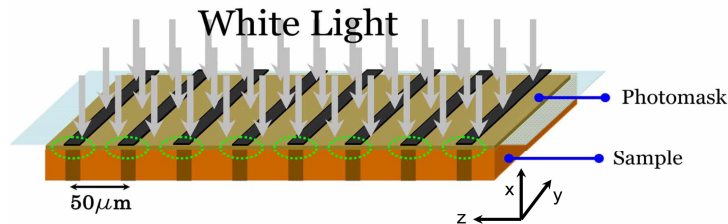


Fig. 2. Schematic plot of white-light induced planar waveguides. The dashed circles show the position of the channel waveguides.

In a second step, white light from a commercial cold light source (IL-FOI, Focus Instrument Co. Ltd., China, with a halogen bulb, Philips Focusline 100W), which is additionally collimated using a convex lens to generate a nearly parallel beam, is used to selectively illuminate the planar waveguide surface through a photo mask (which is in close contact with the sample surface), forming longitudinal photo-induced index stripes. The temperature increase of the sample due to illumination is rather low, thus thermal fixing of written index structures (becoming effective at temperatures above 100°C only) may be neglected. The lithographic mask contains a series of 50 μm -wide periodic patterns, i.e., 10 μm -wide Cr straight stripes (non-transparent to white light) separated by 40 μm -wide transparent regions. Figure 2 depicts a schematic plot of the white light illumination process on top of the sample surface. The exposure time of the planar waveguide is typically set to be 30-60 min. In this way, well-defined regions of the sample are exposed by white light. Consequently, because of the self-defocusing photovoltaic nonlinearity of LiNbO₃, the refractive index will experience negative modifications of Δn_e in a range of -0.0004 to -0.001 (measured by prism-coupling method at 632.8 nm). At the same time, the refractive index in regions protected by the non-transparent Cr stripes remains unchanged. After such illumination for a certain time, the longitudinal shadowed stripes resemble vertical planar waveguides, resulting in non-diffractive light propagation along these stripes, however, only for a limited propagation length. From microscopy investigations [see also Fig. 3(b)] we can conclude that these narrow stripes can preserve their transversal shape down to the substrate for at least 30 μm . As a result of this fabrication, channel waveguides are expected to be formed as a superposition of two planar waveguides, oriented rectangular to each other, in the regions of the ion implanted planar waveguide and the part un-exposed to white light.

In Fig. 3 we show both, top view (a) and transverse cross sections (b), of the fabricated sample imaged by a microscope with reflected polarized light (Olympus BX51M, Japan). As one can see, the top view image of the sample surface clearly shows stripes induced by the white illumination, and the cross section photograph indicates the formation of channel

waveguide as a result of the superposition of the two planar waveguides: lateral ion implanted waveguide and the longitudinal white-light illuminated dark-soliton-like structures.

For numerical modeling of the fabricated structures, the 2D refractive index distributions of the channel waveguide cross sections are reconstructed by considering the longitudinal (along x -axis) planar waveguide index profile and the lateral (along z -axis) index modulations induced by the white light illumination, i.e., a superposition of the index changes of O^{3+} ion implantation and the photo-induced index perturbation. Figure 4 shows the three dimensional (3D) plot of the 2D index distribution of the channel waveguide cross section.

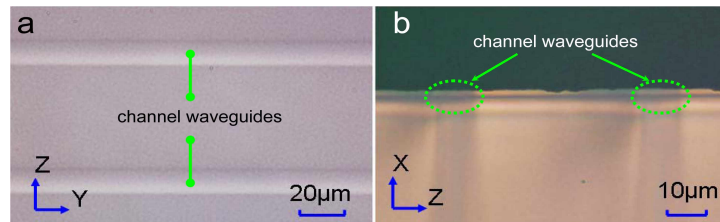


Fig. 3. Microscopic images of (a) top view and (b) transverse cross sections of the sample.

To investigate the transmission properties of the channel waveguides, we use an end-face coupling arrangement by launching a light beam with wavelength of 632.8 nm from a linearly polarized He-Ne laser (similar to the setup in [18]). Figures 5(a) and 5(c) show the near-field intensity distributions of the light in the TE_{00} and TE_{10} modes, respectively. Different from former results where coherent laser beams have been used [18], here the white light induces multi-mode waveguides. As we can see, the light can be guided in a well confined way without leakage through the implanted index barrier. For tailoring the light guiding properties of the light-induced structures, it is helpful to model the light propagation in the channel waveguides. For such a purpose, we apply a numerical simulation of the light propagation of the photo-induced channel waveguides, based on the finite difference beam propagation method (FD-BPM) [29], using a commercial software [30]. The 2D refractive index distribution shown in Fig. 4 is used to characterize the channel waveguides. Figures 5(b) and 5(d) depict the modal distributions of TE_{00} and TE_{10} modes, respectively. Here the excitation of the higher mode TE_{10} is performed, similar as in the experiment, by using a Gaussian input beam laterally shifted with respect to the symmetric input condition used to excite the fundamental mode TE_{00} . By comparing Figs. 5(a) and 5(c) (experimental intensity profiles) with 5(b) and 5(d) (calculated modal intensity profiles), one may conclude that there is a fairly well agreement between numerical and experimental data, which allows for the modeling of tailored channel waveguide structures through the induction of white light.

The channel waveguides induced by white light can be pretty stable against optical erasure up to optical intensities of $\sim 5W/cm^2$ at the used wavelength of 632.8 nm. However, it should be pointed that at communication wavelength bands (1.3 and 1.5 μm) the photorefractive effect in $LiNbO_3$ is almost negligible [31], and hence such waveguides could remain superior stability at much high intensities in the near-infrared range. Another important feature of the channel waveguides is that the white-light induced patterns can be erased by homogenous white light illumination over the sample surface. By using white light from the same lamp and using the same optical power, the induced index changes in the channel stripes could be completely removed within 30 min, allowing for easy reconfiguration of channel waveguide devices. On the other hand, without such illumination, the relaxation time of light-induced structures is of the order of a few weeks in our samples used here, but may be further increased up to a few years in optimized $LiNbO_3$ crystals having very low dark conductivity.

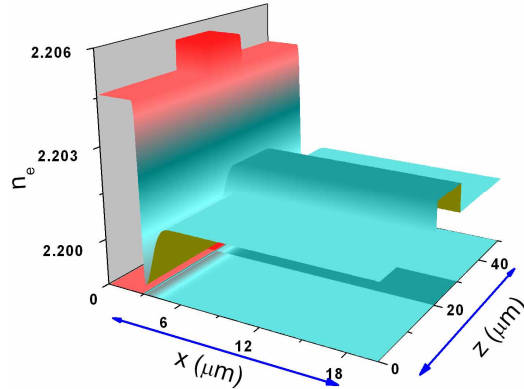


Fig. 4. 3D plot of the 2D index profile of the white light induced channel waveguide on top of O^{3+} ion implanted planar waveguide.

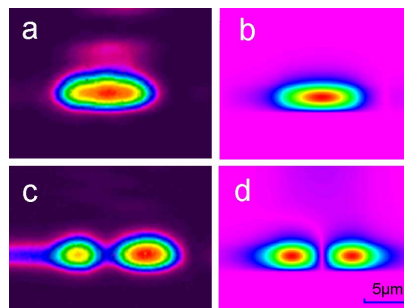


Fig. 5. Experimentally measured near-field intensity distribution of channel waveguide modes (a) TE_{00} and (c) TE_{10} , and related numerically calculated modal profiles [(b) and (d)] using BeamPROP software. The used wavelength of both experiment and simulation is 632.8 nm.

3. Conclusion

Optically reconfigurable channel waveguides have been produced by selective white-light illumination through a specially designed photo mask on top of a low-dose O^{3+} ion implanted Fe:LiNbO₃ planar waveguide substrate. The illumination of white light induces negative refractive index changes in the exposed regions, while the non-illuminated regions experience negligible index modifications, forming longitudinal non-diffractive structures superimposed on the ion-implanted planar waveguide host. Together with the lateral confinement, reconfigurable channel waveguides are formed in the overlap regions. The numerical simulations show good agreement with the experimental results, exhibiting promising potentials for LiNbO₃ waveguide devices in the infrared wavelength bands, at which the materials' photorefractive is negligible.

Acknowledgments

This work is carried out with the financial support of National Natural Science Foundation of China (NSFC, Project 10505013), NSFC-RFBR (Project 10711120169), RFBR (Project 06-02-39017), and Ministry of Science of Republic Serbia (Project 141034). FC also thanks SRF for ROCS, SEM.